Supplementary Information

MoS_2@MWCNT Modified Glassy Carbon Electrode for Electrochemical Mercury (II) Ion Sensor

Jai Mishra[a], Nipun Sharma[b], Sumit Kumar[a], Chayan Das[c], Amit Kumar[a],Monika Kwoka[d], Satyjit Sahu[c], Mahesh Kumar[a,b*]

[a]*Department of Electrical Engineering, Indian Institute of Technology Jodhpur, Jodhpur 342030, India.*
[b]*Interdisciplinary Department of Space Science and Technology, Indian Institute of Technology Jodhpur, Jodhpur 342030, India.*
[c]*Department of Physics, Indian Institute of Technology Jodhpur, Jodhpur 342030, India.*
[d]*Department of Cybernetics, Nanotechnology and Data Processing, Faculty of Automatic Control, Electronics and Computer Science, Silesian University of Technology, Akademicka 16, 44-100 Gliwice, Poland*
[*]Corresponding author: mkumar@iitj.ac.in

S.1. EDX Mapping Image of MoS_2@MWCNT

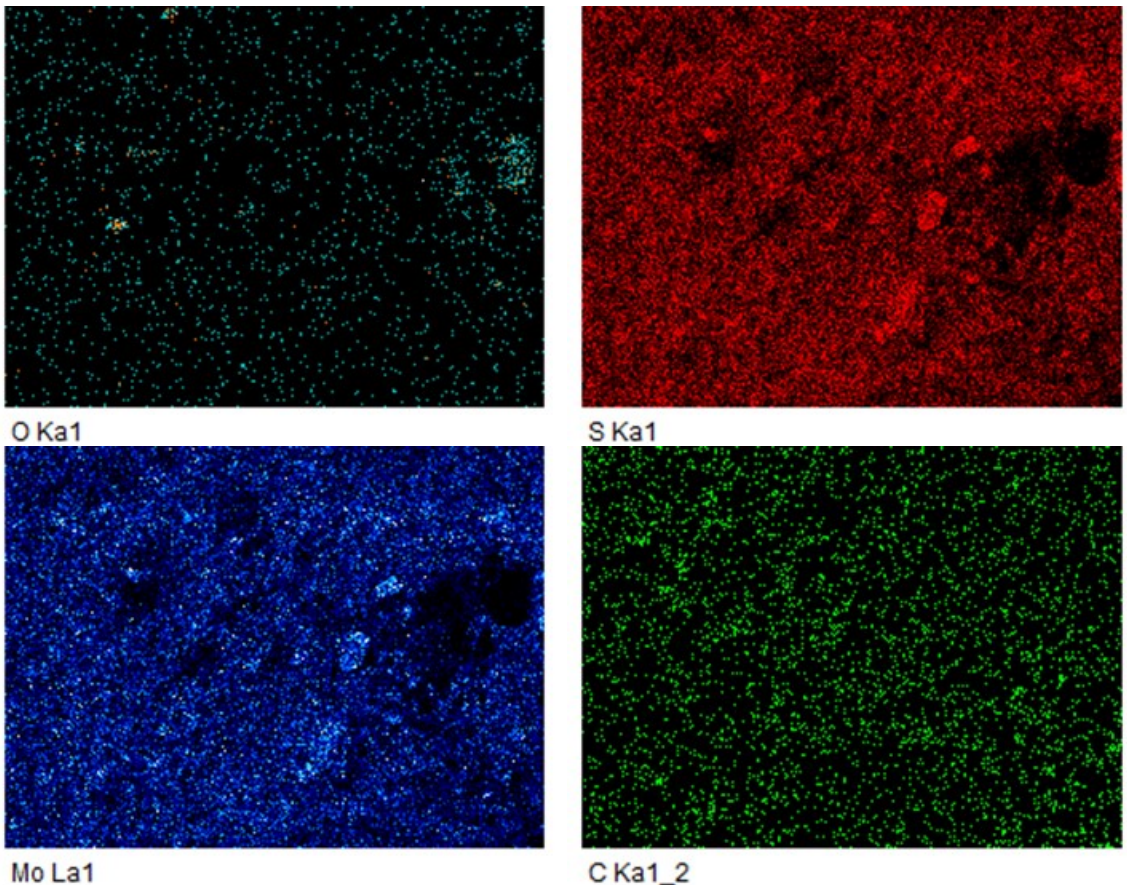

Fig. S1 EDX Mapping Image of MoS_2@MWCNT

S.2. CV response of MWCNT/GCE

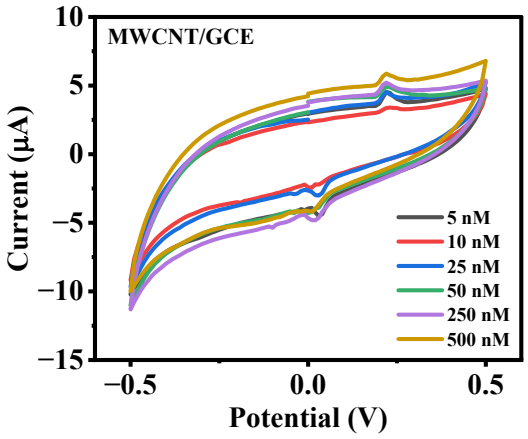

Fig. S2 CV response of the MWCNT/GCE with the increasing concentration of Hg^{2+} (5 nM to 500 nm) in 1 M PBS at a scan rate of 100 mVs^{-1}.

S.3. Optimization Study

To enhance the performance of the MoS_2@MWCNT composite sensor for mercury detection, a series of optimization studies were conducted. Key parameters such as buffer pH, temperature, deposition potential, and deposition time were systematically investigated to determine their effects on sensor sensitivity and response. To verify the applicability of the MoS_2@MWCNT sensor under the real environmental conditions, the studies have been extended to different pH and temperature conditions. For pH studies, 0.1 M PBS buffer was chosen as the electrolyte, to keep the pH stable during the experiments. The studies show variations in the current response with pH from 3–10 in **Fig. S3 b**, and there is a measurable current response at all pH values in the studied electrolyte conditions. Similarly, the response of the MoS_2@MWCNT/GCE for different temperatures of the testing solution (20-50 °C) was recorded Fig. S3 d). The current increase observed with the increase in the temperature shall be ascribed to the increase in the reaction rate with temperature and due to the increase in the mobility of ions. Thus, the results show that the sensing of Hg^{2+} using MoS_2@MWCNT is feasible at all pH and at temperature range (20 °C and at a higher temperature of 50 °C and beyond), showing its applicability under the environmental conditions.

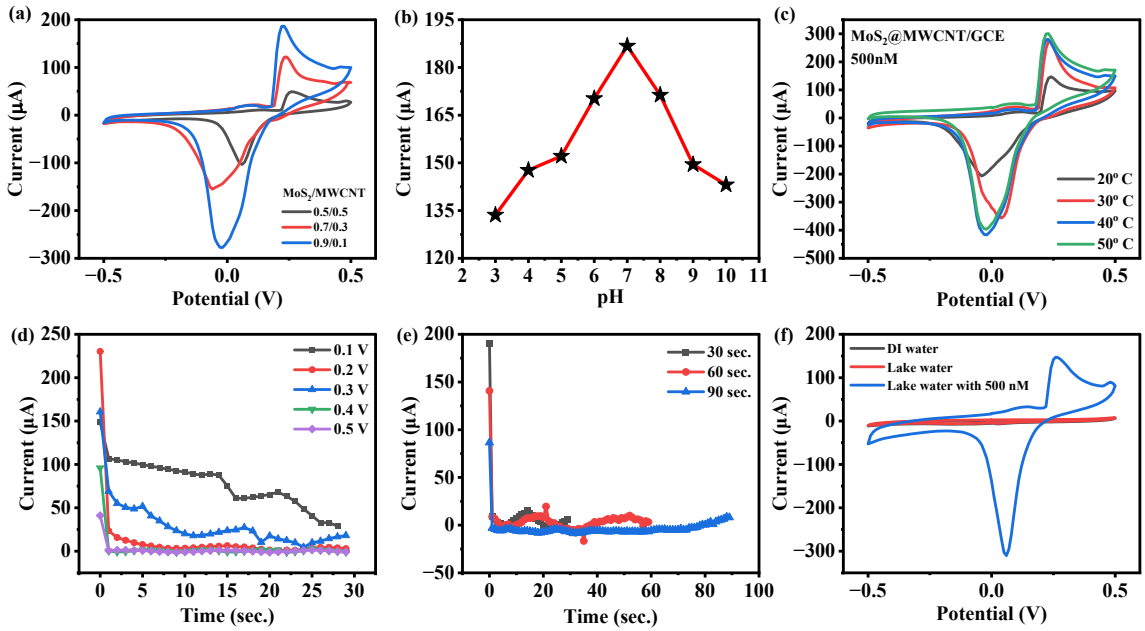

Fig. S3 (a) CV response of MoS_2@MWCNT /GCE with varying ratios of the compositions in 500 nM Hg^{2+} in 1 M PBS at a scan rate 100 mVs^{-1} (b) buffer pH, (c) Temperature, Chronoamperometric study for MoS_2@MWCNT for (d) deposition potential in range from (0.1 V to 0.5 V), (e) deposition time, (f) CV response for real time sensing.

To identify the optimal deposition potential for mercury detection using the MoS_2@MWCNT composite, a chronoamperometric deposition study was performed by applying potentials ranging from 0.1 V to 0.5 V. At each applied potential, a sharp initial increase in current was observed, representing the rapid oxidation of mercury ions onto the electrode surface. As the potential increased from 0.1 V to 0.5 V, the magnitude of the initial current spike increased, indicating a stronger driving force for electron transfer and oxidation at higher potentials. Following the initial spike, the current decayed over time, transitioning from a kinetically controlled regime to a diffusion-controlled regime. The current eventually stabilized, with steady-state values corresponding to the diffusion of mercury ions to the electrode surface.

S.4. Reversibility Study

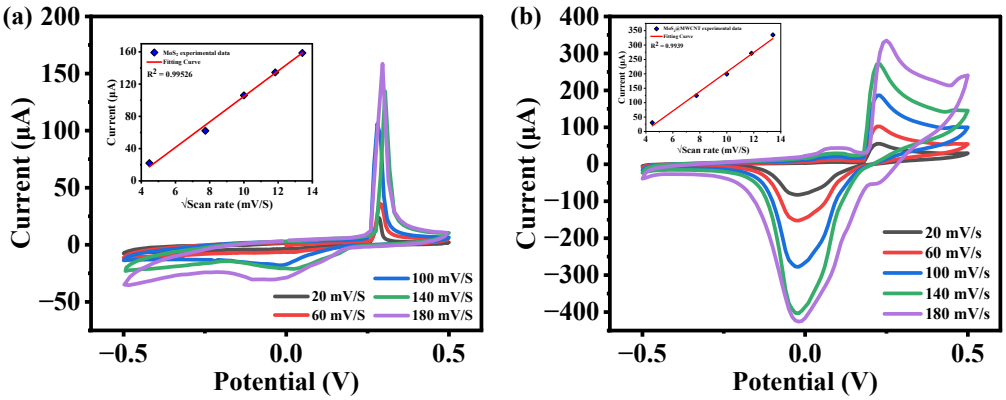

Fig. S4 Cyclic voltammograms of MoS_2/GCE (a) and MoS_2@MWCNT/GCE (b) with various scan rates from 20 to 180 mV/s. Anodic peak currents vs. square root of scan rate for of MoS_2/GCE (a inset) and MoS_2@MWCNT/GCE (b inset).

S5. Selectivity, Stability and Reproducibility study

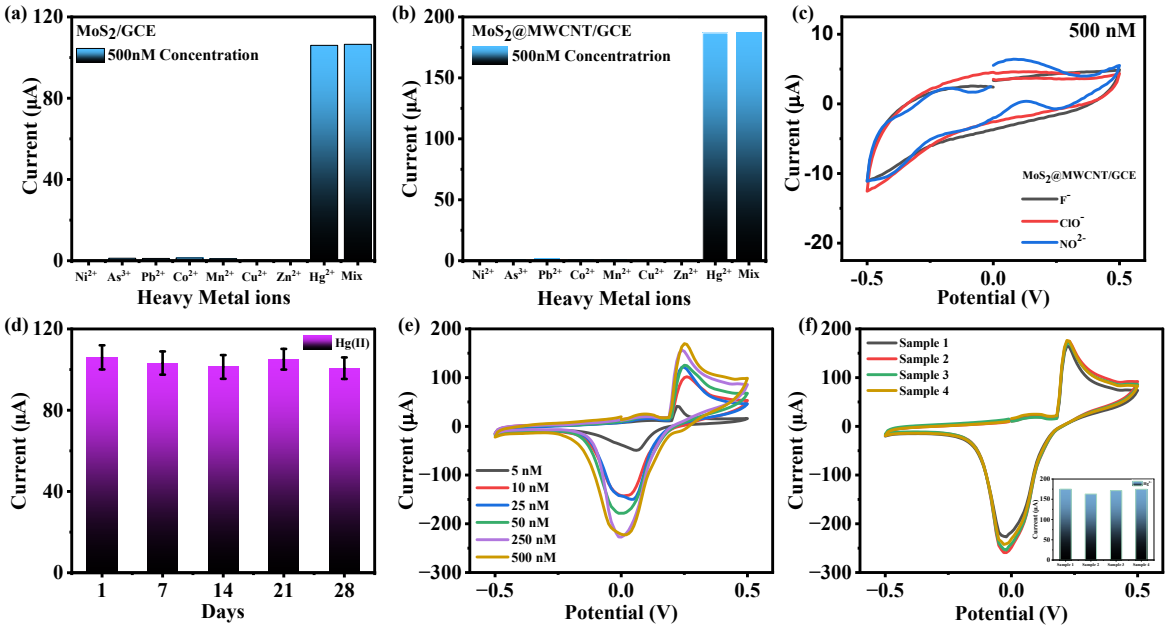

Fig. S5. Selectivity test bar graph of the (a) MoS_2, (b) MoS_2@MWCNT-modified electrodes towards Hg^{2+} ions in the presence of various competing metal ions (Ni^{2+}, As^{3+}, Pb^{2+}, Co^{2+}, Mn^{2+}, Cu^{2+}, and Zn^{2+}) (c) CV representation with different anions at 500 nM concentration. (d) MoS_2 – stability, MoS_2@MWCNT (e) Reproducibility (f) Batch to batch study at 500 nM concentration.

Table S1. Comparison of the MoS_2@MWCNT/GCE with Previously Reported Electrodes for the Detection of Hg^{2+}.

S. No.	Functional Units	Linear range	LoD	Electrode	Ref.
1.	*MoS_2-rGO*	*0.1–10 µM*	*1.6 µM*	*CPE*	[1]
2.	*Ag-rGO*	*0.01–100 µM*	*0.0049 µM*	*GCE*	[2]
3.	*Au/MoS_2-MWCNT*	*0.1 nM–1 µM*	*0.05 nmol*	*GCE*	[3]
4.	*N, S-carbon/Sep*	*0.4–85 µM*	*0.1 µM*	*CPE*	[4]
5.	*$Zn_3(PO_4)_2$@MWCNTs/DNA*	*0.1 nM–50 nM*	*0.07 nM*	*-*	[5]
6.	*H_2bpabza/MWCNT*	*9.97 to 697.94 µM*	*1.5 µM*	*GCE*	[6]
7.	*MoS_2@MWCNT*	*5 nM – 500 nM*	*2 nM*	*GCE*	*This Work*

References

1 D. S. Rana, R. Sharma, S. Kumar, N. Gupta, S. Thakur, K. K. Thakur and D. Singh, *Nano-Structures \& Nano-Objects*, 2023, **36**, 101041.

2 S. Ma, Q. Zhang, J. Zhu, H. Shi, K. Zhang and Y. Shen, *Sensors Actuators B Chem.*, 2021, **345**, 130383.

3 A. Mohammadi, E. Heydari-Bafrooei, M. M. Foroughi and M. Mohammadi, *Microchem. J.*, 2020, **158**, 105154.

4 M. Ghanei-Motlagh and M. Baghayeri, *Mater. Chem. Phys.*, 2022, **285**, 126127.

5 L. He, S. Zhang, M. Wang, D. Peng, F. Yan, Z. Zhang and L. Zhou, *Sensors Actuators B Chem.*, 2016, **228**, 500–508.

6 K. S. Selvan, G. Jayagopi and S. Sivalingam, *(Mater. Adv., 2024, Advance Article)(10.1039/D4MA00335G)*